

Dependence of Depolarization on Incident Polarization for 19-GHz Satellite Signals

BY H. W. ARNOLD and D. C. COX

(Manuscript received July 20, 1978)

Rain and ice crystals depolarize radio waves along earth-satellite propagation paths. The magnitude of this depolarization is a function of incident polarization angle and is minimized when polarization and depolarizer symmetry axes coincide. A technique is presented for a direct determination of the medium's attenuation and depolarization for any incident polarization, based on measurements taken at two orthogonal polarizations. Some sample results from this technique are presented, using data collected at Crawford Hill, New Jersey using the 19-GHz COMSTAR satellite beacon.

I. INTRODUCTION

Depolarization caused by rain and ice crystals is an important factor in the design of future satellite communication systems operating at frequencies above 10 GHz.^{1,2} These systems will likely use dual, orthogonal polarizations to increase transmission capacity. Quantitative knowledge of depolarization is necessary for determining the pair of polarizations that experience the least depolarization, for determining whether the isolation between any two polarizations is adequate during rain and ice depolarizing conditions, or for guiding the design of circuits for canceling crosstalk resulting from depolarization if the isolation is not adequate.

Only a few measurements have been made of depolarization along earth-space propagation paths.³⁻⁵ These measurements were not necessarily made at incident polarizations that produce minimum depolarization. Aerodynamic forces acting on vertically falling raindrops are expected to orient raindrop symmetry axes vertical and horizontal on the average. Thus, rain depolarization is expected to minimize at linear horizontal and vertical polarizations. Maximum depolarization is expected for linear polarizations oriented 45 degrees to horizontal and for circular polarizations.^{5,6} These expectations are supported by mea-

surements for terrestrial propagation paths, but there is no experimental evidence available to either confirm or refute them for earth-space paths. Depolarization caused by ice crystals with unknown orientations raises additional uncertainty in the expected behavior of depolarization along earth-space paths.⁷

It is difficult and expensive to instrument satellites to measure depolarization directly at several incident polarizations. A technique involving direct measurement of elements in the polarization transmission matrix and direct calculation of depolarization for other incident polarizations was proposed for the COMSTAR beacon propagation experiments.^{8,9} This calculation method has the potential for answering many of the questions regarding rain and ice depolarization along earth-space propagation paths. This paper presents what are believed to be the first experimental results obtained using the technique.¹⁰ A minimum in depolarization occurs for vertical and horizontal incident polarizations for the attenuation event analyzed.

II. THE MEASUREMENTS

2.1 *Equipment and signal parameters*

The transmitting source for the propagation measurements is the 19-GHz beacon¹¹ on the COMSTAR satellite located at 95°W longitude. This beacon output is switched at a 1-kHz rate between two linear orthogonal polarizations. These 19-GHz signals, among others, are received at Crawford Hill, New Jersey with a 7-m diameter antenna and precision receiving electronics described in Refs. 12 and 13.

The polarizations of the beacon signals received at Crawford Hill are rotated 21 degrees from horizontal and vertical (for simplicity, these signals are referred to as H and V). Amplitudes of copolarized, V and H, and cross-polarized, XV and XH, signal components are measured for the two transmitted polarizations. Phase differences, ϕ , referenced to the V signal are measured for the H, XV, and XH signals. The receiver 3-dB predetection bandwidths of 10 Hz in co- and crosspolarized channels yield a dynamic range of 60 dB between the clear air copolarized signal level and the receiver noise level; crosspolarized signal amplitudes are also measured in 1-Hz bandwidths yielding a 70-dB dynamic range. Post-detection bandwidths are 1 Hz for all amplitude and phase measurements.

Residual signals in the crosspolarized signal channels are produced by transmitting and receiving antenna imperfections. These residuals are <-35 dB below the copolarized signal levels everywhere within the -3 dB beamwidth of the receiving antenna. Residuals are <-40 dB everywhere within the beam for the XV channel (XV is the channel for transmit vertical and receive horizontal); on-axis residuals are typically <-45 dB for XV and -36 to -40 dB for XH.

2.2 Calibration

The crosspolarized signal channels are calibrated with the antenna feed in the normal receiving position. The receiver polarization switches (see Figs. 1 and 14 of Ref. 13) are temporarily configured to connect the H and V copolarized signals through the XV and XH channels respectively. These known signal levels are then used to establish the gains of the crosspolarized signal channels. These channel gains remain within ± 0.1 dB over many months. The H and V signals are within 0.05 dB of each other as measured by physically rotating the receiving antenna feed assembly 90 degrees. The phase scale for the differential phase, $\phi V-H$, is calibrated by reversing the polarity of one signal input to produce a 180-degree phase change.

Determination of the zero on the phase scales for the crosspolarized signals, $\phi V-XV$ and $\phi V-XH$, requires simultaneous insertion of signals with known phase relationship into the receiving feeds. Rotating the feed assembly inserts projected spatial components of the copolarized signals into both feeds. These components have the same phase and will produce signals with either 0- or 180-degree phase difference in the crosspolarized signal channels; the sense, 0 or 180, depends on the direction of feed rotation. Contamination by the residual crosspolarized signals produces an uncertainty in this zero of about ± 1 degree. This zero calibration remains within ± 2 degrees over many months. The phase scale is calibrated by reversing the polarity of one signal input while rotating the feed assembly for the zero determination. Note that the phases of the clear-air residual crosspolarized signals are not suitable for determining phase scale and zero because they are low level and their phases are extremely sensitive to the accuracy of the nulling of the residuals with feed assembly rotation.⁷

2.3 Baseline removal

The amplitudes and phases of co- and crosspolarized beacon signals exhibit small diurnal variations. These diurnal baseline variations repeat very closely from day to day, but change somewhat from season to season. The variations result from thermal changes in the satellite beacon circuits, waveguides, and antennas as the solar illumination changes. Day-to-day receiver contributions to baseline variations are insignificant. Because of the repeatability of these baseline variations, they can be removed from the experimental data.

V and H attenuations and differential phase, $\phi V-H$, are determined by subtracting, from values measured during propagation events, the values measured at the same clock times on clear days within a few days of the events. The differential values of attenuation and phase that are critical in the calculation of depolarization for other incident polarizations are determined within ± 0.2 dB and ± 0.5 degree.

Baseline removal of residual crosspolarized components is done by vectorially subtracting, from the values measured during events, the weighted residual components at the same clock times. These vector subtractions can be made since both amplitudes and phases are measured. Prelaunch measurements of the beacon antennas, pattern range measurements on the receiving antenna, and measurements with the receiving feed at normal polarization and rotated 90 degrees all suggest that the XH residual is dominated by the beacon antenna. Thus, the XH residual is weighted by the event attenuation and differential phase as though it were all contributed by the beacon. Weighting of the XV residual assumes equal contribution by beacon and receiving antennas. The vector subtraction of clear-air crosspolarized channel residuals suppresses the residuals to -45 to -50 dB below copolarized signal levels before and after events and on adjacent clear days. This accuracy degrades with the intensity of the propagation event because of the uncertainty in assigning residual contributions to beacon and receiving antennas. However, during weak events when depolarization is low and residual suppression is needed, the residual is suppressed to -45 to -50 dB; when the event is stronger and the suppression degrades, the depolarization is strong and the relative errors contributed by the residual are less significant anyway.

III. POLARIZATION ROTATION TECHNIQUE

This section introduces the concept of the medium transmission matrix for a given set of incident and received polarizations. Receiver outputs directly generate the transmission matrix for the incident polarizations; results for other incident polarizations are generated through rotations of the measured matrix.

Let us assume two orthogonal signals, E_{Ta} and E_{Tb} , incident on the medium. The medium outputs in the same reference frame are E_{Ra} and E_{Rb} . The medium is then completely described by four coupling coefficients, as shown in Fig. 1. Coefficients A and D represent the copolarized signal attenuations of the medium, while B and C indicate the medium's depolarization. Note that these coefficients are, in general, complex. The above relation may be written in matrix form:

$$\begin{bmatrix} E_{Ra} \\ E_{Rb} \end{bmatrix} = \begin{bmatrix} A & B \\ C & D \end{bmatrix} \begin{bmatrix} E_{Ta} \\ E_{Tb} \end{bmatrix}. \quad (1)$$

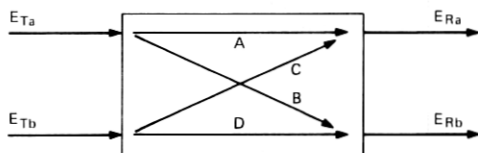


Fig. 1—Description of propagation medium by coupling coefficients A , B , C , D (E_{Ta} and E_{Tb} transmitted, E_{Ra} and E_{Rb} received).

Since the 19-GHz COMSTAR beacon transmits alternately on two orthogonal polarizations, E_{T_a} and E_{T_b} are alternately 0. Receiver outputs^{8,13} are thus directly proportional to A and C (for $E_{T_b} = 0$) or B and D ($E_{T_a} = 0$). The transmission matrix T_M for the actual incident polarizations is given by these measured values.

$$[T_M] = \begin{bmatrix} A_M & B_M \\ C_M & D_M \end{bmatrix}. \quad (2)$$

This measured transmission matrix may now be used to generate the transmission matrix for any other orthogonal set of incident polarizations. This operation is done without recourse to path models. Linear, circular, or elliptical polarizations are admissible; the following discussion considers only linear polarization. As shown in Fig. 2, the transmission matrix for the 1-2 frame is desired, based on measurements obtained in the $M_a - M_b$ frame. Components in the 1-2 frame are obtained from those in the $M_a - M_b$ frame through the following relation:

$$\begin{bmatrix} E_1 \\ E_2 \end{bmatrix} = [R_\theta] \begin{bmatrix} E_{M_a} \\ E_{M_b} \end{bmatrix}, \quad (3)$$

where

$$[R_\theta] = \begin{bmatrix} \cos \theta & -\sin \theta \\ \sin \theta & \cos \theta \end{bmatrix}. \quad (4)$$

To generate the transmission matrix for incident polarizations along the 1-2 axes, the 1-2 inputs are rotated into the measurement frame by $[R_\theta]$, passed through the transmission matrix $[T_M]$, and rotated back to the 1-2 frame by $[R_\theta]^{-1}$, i.e.,

$$\begin{bmatrix} E_{R1} \\ E_{R2} \end{bmatrix} = [R_\theta]^{-1} [T_M] [R_\theta] \begin{bmatrix} E_{T1} \\ E_{T2} \end{bmatrix}. \quad (5)$$

The transmission matrix $[T_{M,\theta}]$ for two orthogonal polarizations rotated an angle θ from the measurement frame is thus

$$[T_{M,\theta}] = [R_\theta]^{-1} [T_M] [R_\theta]. \quad (6)$$

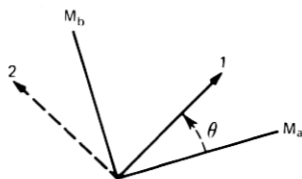


Fig. 2—Relation between reference frames of measured ($M_a - M_b$) and desired (1-2) transmission matrices.

IV. OBSERVATIONS

The accuracy of the polarization rotation technique described here is critically dependent on amplitude and phase calibration of all four receiver channels.⁹ To verify the end-to-end operation of the receiver and rotation software, a depolarizer with known symmetry axes was inserted near the receiving antenna focus in clear weather. Data were taken at several orientations of the depolarizer with respect to the actual received polarizations. For each case, depolarization was computed as a function of incident polarization angle relative to the depolarizer symmetry axes. All results were identical, with minimum depolarization along the depolarizer symmetry axes. This agreement validates both the receiver calibration and rotation software.

Data from a recent rainstorm were analyzed to determine the dependence of depolarization and attenuation on incident polarization angle. Since little depolarization was observed before or after the high-attenuation portion of the event, it appeared that rain, rather than ice, was the predominant depolarizing agent.^{7,10}

Some effects of incident polarization angle are shown in Fig. 3 for three points in this storm. These points had maximum vertical copolarized attenuations of 5.4, 10.4, and 20.3 dB. The lower three curves show the effect of vertical depolarization (the ratio of vertical crosspolarized to copolarized levels) as a function of polarization rotation from local ver-

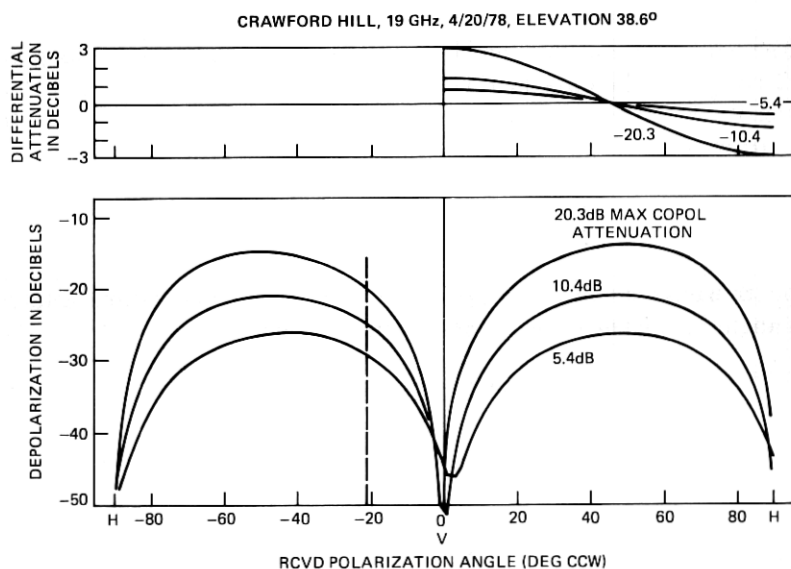


Fig. 3—Variations in depolarization and differential attenuation with incident polarization angle for three points during April 20, 1978 rainstorm. Solid curves are calculated from measurements made at an incident polarization of -21 degrees indicated by the dashed line.

tical to horizontal. The experimental data, taken at a 21-degree rotation angle, appear along the dashed line. All three curves exhibit a sharp null within 2 degrees of local vertical, indicating a mean raindrop canting angle close to 0 degree.^{5,6,10}

The upper three curves indicate the variation in differential attenuation (the ratio of horizontal to vertical copolarized attenuations) with polarization angle. Maximum differential attenuation coincides with minimum depolarization, since the raindrops then exhibit their maximum oblateness along the two incident polarizations. Differential attenuation changes sign at 45 degrees from this point, as "vertical" and "horizontal" interchange roles.

The temporal history of a portion of this rainstorm is shown in Fig. 4. The upper two curves indicate maximum depolarization (for 45-degree polarization) and the concurrent copolarized attenuation. A maximum depolarization of -11 dB was observed at 30-dB copolarized attenuation. Maximum depolarization exceeded -20 dB for all copolarized attenuations exceeding 11 dB.

The lower curves indicate time variations for polarization angles in the vicinity of the nulls shown in Fig. 3. The central curve indicates the polarization angle exhibiting minimum depolarization, while the outer curves show the -20 and -30 dB depolarization contours around this

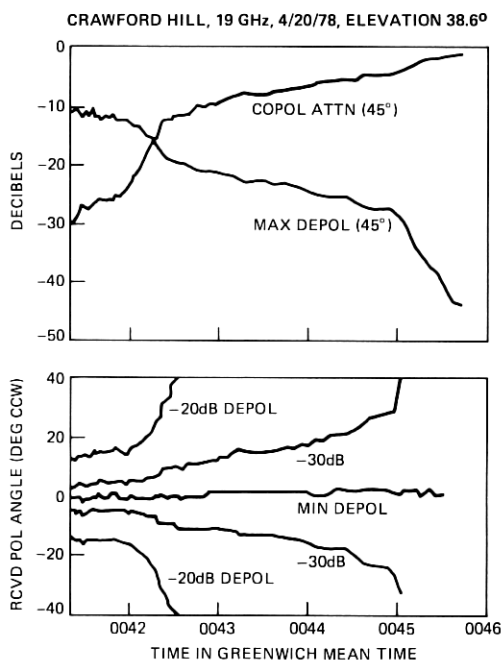


Fig. 4—Temporal history of portion of April 20, 1978 rainstorm. Upper curves show copolarized attenuation and maximum depolarization. Lower curves show angular location and extent of depolarization minima.

minimum. For this portion of this event, the polarization angle exhibiting minimum depolarization remained within 2 degrees of local vertical. Depolarization remained below -30 dB for all polarizations within 3.5 degrees of local vertical, and below -20 dB within 12 degrees of local vertical.

The relation between attenuation and depolarization appeared to be well-behaved for the section shown of this rainstorm. Other regions, however, appeared less homogeneous. Figure 5 shows the polarization angle dependence of depolarization and differential attenuation for two points in the storm separated by 19 minutes. Both points had 10.5-dB copolarized attenuation. The earlier point, however, had 2.5-dB lower maximum depolarization, almost 50 percent lower differential attenuation, and more than 50 percent greater maximum differential phase shift between copolarized channels. In addition, the depolarization null was filled in below -41 dB. All these changes are consistent with lower average raindrop ellipticity (or less preferential drop orientation) and the presence of a small amount of depolarization due to ice crystals.^{7,10} Very preliminary observations of other events have suggested that depolarization nulls occasionally deviate far from local vertical during periods of predominantly ice depolarization.

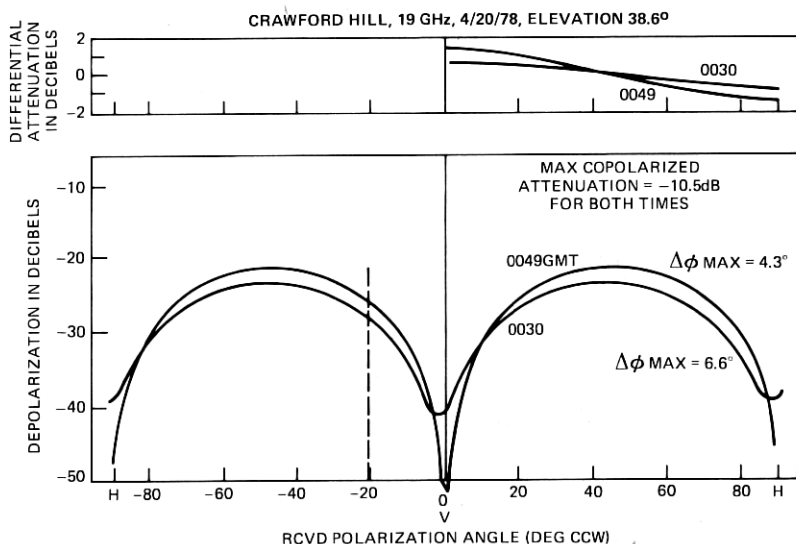


Fig. 5—Variations in depolarization and differential attenuation with incident polarization angle for two points in April 20, 1978 rainstorm exhibiting identical copolarized attenuation but different depolarization characteristics. Solid curves are calculated from measurements made at an incident polarization of -21 degrees indicated by the dashed line.

V. CONCLUSIONS

A method has been presented, based on transmission measurements at one set of incident polarizations, for direct calculation of attenuation and depolarization of the transmission medium for any incident polarization. This technique has been applied to 19-GHz data from the Crawford Hill COMSTAR beacon propagation receiver. Test results indicate that the receiver calibration accuracy is sufficient to provide useful information on polarization-dependent effects along earth-space propagation paths.

The rainstorm analyzed exhibited a sharp depolarization minimum for incident polarizations within 2 degrees of vertical and horizontal. This implies that the mean raindrop symmetry axis was nearly vertical. The minimum depolarization was sufficient for communication systems employing polarization reuse.

Similar observations of ice-produced depolarization events suggest that the depolarization minima for these events occur occasionally at polarizations other than vertical and horizontal. This implies ice particle alignment by other than gravity. The simultaneous presence of ice and rain with differing symmetry axes could destroy the depolarization nulls observed with either separately. Such events, if frequent, could have a serious impact on dual-polarization communication systems. The technique described here will allow further investigation of this and other polarization-dependent propagation phenomena on earth-space paths.

REFERENCES

1. D. O. Reudink, "A Digital 11/14 GHz Multibeam Switched Satellite System," AIAA/CASI 6th Communication Satellite Systems Conference, Montreal, April 5-8, 1976.
2. L. C. Tillotson, "A Model of a Domestic Satellite Communication System," *B.S.T.J.*, 47, No. 10 (December 1968), pp. 2111-2137.
3. D. A. Gray, Fig. 35 in ref. 5.
4. A. J. Rustako, Jr., "An Earth-Space Propagation Measurement at Crawford Hill Using the 12-GHz CTS Satellite Beacon," *B.S.T.J.*, 57, No. 5 (May-June 1978), pp. 1431-1448.
5. D. C. Hogg and T. S. Chu, "The Role of Rain in Satellite Communications," *Proc. IEEE*, 63 (September 1975).
6. T. S. Chu, "Rain-Induced Cross-Polarization at Centimeter and Millimeter Wavelengths," *B.S.T.J.*, 53, No. 8 (October 1974), pp. 1557-1579.
7. D. C. Cox, H. W. Arnold, and H. H. Hoffman, "Depolarization of 19- and 28-GHz Earth-Space Signals by Ice Particles," *Radio Science*, 13 (May-June 1978).
8. D. C. Cox, "Design of the Bell Laboratories 19- and 28-GHz Satellite Beacon Propagation Experiment," *IEEE International Conference on Communications (ICC '74) Record*, June 17-19, 1974, Minneapolis, Minnesota, pp. 27E1-27E5.
9. D. C. Cox, "Some Effects of Measurement Errors on Rain Depolarization Experiments," *B.S.T.J.*, 54, No. 2 (February 1975), pp. 435-450.
10. D. C. Cox and H. W. Arnold, "COMSTAR Beacon Measurements at Crawford Hill: Attenuation Statistics and Depolarization," *USNC/URSI Spring Meeting*, May 15-19, 1978, University of Maryland, College Park, Maryland.
11. D. C. Cox, "An Overview of the Bell Laboratories 19- and 28-GHz COMSTAR Beacon Propagation Experiments," *B.S.T.J.*, 57, No. 5 (May-June 1978), pp. 1231-1255.

12. T. S. Chu, R. W. Wilson, R. W. England, D. A. Gray, and W. E. Legg, "The Crawford Hill 7-Meter Millimeter-Wave Antenna," *B.S.T.J.*, 57, No. 5 (May-June 1978), pp. 1257-1288.
13. H. W. Arnold, D. C. Cox, H. H. Hoffman, R. H. Brandt, R. P. Leck, and M. F. Wazowicz, "The 19- and 28-GHz Receiving Electronics for the Crawford Hill COMSTAR Beacon Propagation Experiment," *B.S.T.J.*, 57, No. 5 (May-June 1978), pp. 1289-1329.